5th International Symposium on Hydraulic Structures
Hydraulic Structures and Society: Engineering Challenges and Extremes
ISBN 9781742721156 - DOI: 10.14264/uql.2014.44
Brisbane, Australia, 25-27 June 2014

# Preliminary Investigation of the Tsunami-Borne Debris Impact on Structures: A new method for impact force measurement

S.R. Shafiei[1], B.W. Melville[1], S. Beskhyroun[1] and A.Y. Shamseldin[1]
[1]Department of Civil and Environmental Engineering
The University of Auckland
Auckland City 1010
New Zealand
E-mail: ssha399@aucklanduni.ac.nz

***Abstract:*** *Impact of tsunami-borne debris causes a significant force on coastal structures. Tsunami bores can carry different geometrical shapes of floating debris, which are often the greatest cause of damage to inland structures. Despite such a serious threat, the impact of floating debris on structures has received limited attention. The objective of this paper is to introduce a new method for measuring the impact force of floating debris on the seaward wall of structures during tsunami events. This will improve the understanding of tsunami-borne debris impact forces on structures and increase the predictive capabilities required for estimates of such forces in design guidelines. The debris impact tests were conducted using two smart debris devices with different geometrical shapes. Impact accelerations and forces in the horizontal and vertical planes were investigated.*

***Key words:*** *Impact, smart debris, force, contact point, contact duration, impact angle.*

## 1. INTRODUCTION

Tsunami-borne debris strike structures and, because of the large induced forces, are the greatest cause of damage to inland structures during tsunami events (Ghobarah et al, 2006, Lukkunaprasit & Ruangrassamee, 2008, Saatçioğlu, 2009). Proper quantification of the forces involved in debris impact is vital for design of structures in tsunami prone areas. Seaward walls are the most prone to debris impact because their vertical orientation opposes objects travelling horizontally. Roofs are less likely to be impacted by floating debris due to their inclination and distance from the ground. Side walls are subjected to suction pressures and are also unlikely to be hit by debris. Most residential buildings have timber, concrete or steel frames with external cladding and it is very important to improve knowledge about the impact force of floating debris on claddings and on the whole structure during tsunami events.

The impact force of floating debris has received some attention, particularly the impact of woody debris (Haehnel & Daly, 2004, Matsutomi, 2009, Nouri et al, 2010). The impact force of shipping containers has also been studied by a few researchers (Mizutani et al, 2008, Yeom et al, 2009, Madurapperuma & Wijeyewickrema, 2012). ASCE 7 (2006) and FEMA (2011) have introduced an approach to estimate the debris impact force. Their method considers the impact of two rigid bodies and formulates the impact based on the impulse momentum approach, taking into account the mass of the debris, debris velocity and the contact duration of the impact. Different values of the contact duration are recommended by ASCE7 and FEMA.

In spite of the importance of the impact force of floating debris, few studies have been done to quantify such a large force (Matsutomi, 2009, Thomas, 2010). Debris can be of a variety of geometries in nature but most of the previous studies were on the impact of rectangular shaped debris (e.g., a piece of timber); there is a lack of knowledge about the relationship between debris geometry and impact force (Nouri *et* al, 2010). Contradictory observations have been made about the impact duration associated with debris impact. To estimate debris impact forces on structures for design purposes, the influence of the parameters affecting the impact load need to be determined which are difficult to estimate. The complicated experiments, on which the findings are based, are difficult to translate into parameters for design codes. To overcome these difficulties we propose a different approach – direct measurement of the acceleration of the debris directly, and hence force determination.

## 2. METHODOLOGY

Experiments were conducted in a large wave flume, 14 m long, 1.2 m wide and 0.8 m deep connected to a reservoir 11 m long, 7 m wide and 0.6 m deep. The tsunami bore is generated using a 0.9 m high automatic gate which allows rapid release of the water in the reservoir to generate a bore. The gate is fitted across the full width of the flume, and consists of a vertically-sliding gate and a shutter gate. The sliding gate is opened using a hydraulic lift device, is kept open for 4 seconds, and is then automatically closed. The shutter gate opening is semi-automatic, using an electronic signal device; the shutter gate also remains open for 4 seconds before it is also closed. To measure the bore depth and velocity, five capacitance-type wave gauges, with 2 mm accuracy, were placed along the flume centreline and 20 mm above its floor. The first wave gauge was placed 2.5 m downstream from the gate, with the remaining gauges equally spaced 1.75 m apart over a total distance of 9.5 m downstream from the gate. The average bore velocity was calculated using the recorded time at which the bore impacted each wave gauge. To obtain different bore heights and velocities, two combinations of gate opening height (GO) and reservoir water depth (WL) were used: WL=400-GO=200 mm and WL=600-GO=300 mm, which generated bore heights of 140 and 210 mm with 1.98 and 2.59 m/s velocities, respectively. The 'structure' is a 300×300×600 mm square-based prism, constructed from sheets of 5 mm thick Plexiglas, and placed 10 m from the gate (i.e., 500 mm beyond the final wave gauge).

A 'smart debris' device was used to measure the impact force of the debris. The smart debris device is an object with an attached accelerometer, which can measure the acceleration before and at the instant of impact. This allows direct calculation of the forces acting on the structure at the time of collision. As far as we are aware, such data have not previously been obtained using a 'smart debris' device.

Two different geometrical shapes of floating debris were made from Plexiglas - a disc and a box. The disc has an outer diameter of 200 mm, thickness of 50 mm and mass of 510 g; it was made hollow for easier internal attachment and protection of the accelerometer, and also so that it floats. The box was made with a cross section of 100×100 mm, length of 300 mm and mass of 510 g. The accelerometer is a tri-axial impact accelerometer and data logger (GCDC, model X250-2); it has a mass of 40 g with an enclosure box having dimensions of 25.6×26.5×104 mm. The accelerometer is tightly fastened with a clip to the inside of the debris to ensure it does not move during the impact event and protected from water. Figure 1 illustrates the coordinate systems for both the flume (xyz) and the smart debris (pqr), in which the flume x direction is in the flow direction. Because of space limitation within the smart debris, the accelerometer was oriented within the disc (box) with the q axis (r axis) initially aligned with the flume x axis.

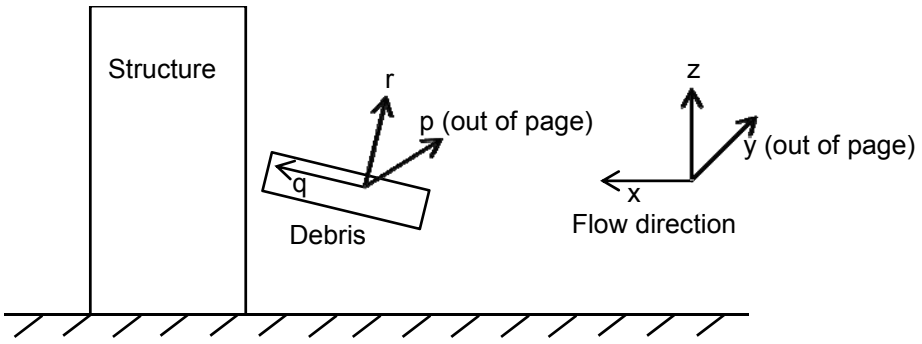


Figure 1 - Coordinate systems for the flume (xyz) and the smart debris (pqr)

The accelerometer is battery powered and USB-rechargeable. The full-scale range of acceleration measurement is ±250 times the standard gravity ($g_n$) in the p, q and r directions, but the sensor also has a non-linear range beyond the rated output, giving an additional range of ±62 $g_n$. It means that, the full-scale range is actually ±(250 + 62) $g_n$, or 625 $g_n$ total. The logger can record samples at up to 512 Hz at 14 bit resolution. The sensors are internally sampled at 16 times this rate, giving an 8192 Hz internal sample rate. The data are then summed and decimated by a factor of 16 to provide a 14 bit effective resolution, in this case 0.0381 $g_n$. The X250-2 typically report less than 1 $g_n$ of noise. The

sensor responds to events with frequency up to about 450 Hz. Records for events with frequency higher than this will be attenuated because the sensor cannot react fast enough. The initial mass of the disc smart debris (disc plus accelerometer plus a chequerboard which is described below) is 560 g. The initial mass of the box smart debris (box plus accelerometer) is 550 g. To conduct the experiment for different masses of debris, an extra 250 g and 450 g of mass were added to the initial mass to get debris with 800 g and 1000 g mass, respectively. The extra mass was added to the centre of the disc; for the box, the extra mass was in four equal pieces that were equally spaced along the long axis. These arrangements were adopted, after various arrangements of extra-mass attachment were trialled during preliminary studies, as those that resulted in the best movement of the smart debris with extra mass. In both smart debris models, the accelerometer was tightly screwed to the body of the debris and as close to the front of the debris as possible, so that movement of the accelerometer did not cause damping of the acceleration.

A 420 fps video camera was used to film the impact, and a floodlight used to improve the video quality. The “Camera Calibration Toolbox for MATLAB” was used to determine the angle of the floating smart debris at the instant of impact. A chequerboard pattern (black and white) was attached to the vertical face of both the structure and the smart debris. The toolbox uses the sub-pixel-accurate corner extraction method to locate the corners of the squares of the chequerboard as they appear in images extracted from video films of the impact. The toolbox finds the sub-pixel corners on the image, based on the Harris corner finder method, to a precision below 0.1 pixel. The method works well as long as the corners of the black and white squares are detectable from the impact snapshot and the deviation of the smart debris from the perpendicular is less than ±5°. An inclined and a vertical line can be fitted to the detected points from the chequerboard attached to the debris and structure, and the angle between the two lines can be calculated using the slopes of the two lines. A 180×80×2 mm sheet of balsa wood was glued to top of the disc and the chequerboard was attached to the sheet. The balsa wood sheet has 10 g mass, light enough to ensure it does not affect the balancing of the disc during its flotation. The chequerboard was attached to the side of the box. The smart debris was placed on the flume floor, 2 m before the structure; it was then carried to the structure by the oncoming bore. The 2 m distance was long enough for the debris to be accelerated to the bore velocity. The debris was washed out immediately after the impact. The impact target is the centre of the structure (‘contact point’); if the debris missed the target, the test was repeated. Also, the test was repeated if the debris deviation from vertical was significant and not suitable for angle detection.

Different velocities of the debris were estimated by integration of the acceleration data over time, which is explained in detail below (in the results section), and utilising video image analysis. The video records were processed in VirtualDub software to get different snapshots of the debris movement. These snapshots were used to obtain the duration of the impact event and also to approximate the average velocity of the debris during the few seconds before impact. For each of the GO-WL and smart debris configurations, experimental tests were repeated ten times to ensure consistency of the results. For each repetition, the entire sequence, from gate opening to backflow from the end wall of the flume, had a duration of about 7 seconds. For each repetition, bore heights and velocities were estimated for each of the four panels formed by the five wave gauges, and averaged to give a bore height and velocity for that repetition. For each configuration, the bore height, the bore velocity, the acceleration, and the force were taken as the means of the values from the five repetitions.

## 3. RESULTS AND DISCUSSION

The smart debris device was not carried by the leading front of the tsunami bore. Initially, the bore front struck the structure, then water rose in front of the structure and splashed upward. The floating debris followed the flow streamlines in front of the structure and consequently collided with the structure at an angle. Figure 2 shows the relation between the experimental configurations (bore velocity and debris mass combinations), and the impact angle (see Section 2). On average, the impact orientation for the disc ranged from 15° to 30° and for the box from 3° to 10°. For the disc, the impact orientation increased with both increasing bore velocity and debris mass, but for the box, there was no apparent relationship between impact angle and these variables. The different rotational movement of the disc and the box result from the different distributions of the extra masses; for the disc it is concentrated in the centre, but in the box it is distributed over the length of the box. The centrally located mass in the disc resulted in magnification of the effect of water fluctuations on the disc motion and resulted in a more random behaviour during the tests. Although the disc and box have almost the

same contact area with the water surface, the longer smart debris (the box) usually impacted the structure at small angles of about 5°, while the disc collided with the structure at a larger angle. This was because of the difference in the contact length of the debris with the water surface, different rotational inertias and possibly mass distribution.

Samples of data collected by the smart debris device (the disc) is shown in Figure 3, for WL= 600 mm and GO= 300 mm and for the mass of 550 g. The impact was in the bore flow direction (q direction for the accelerometer). The first small change in the acceleration relates to the time when the debris was picked up by the bore flow; a few seconds later this rises to a very short duration large acceleration as the debris collides with the structure. The acceleration data were then used to calculate the debris velocity and impact force.

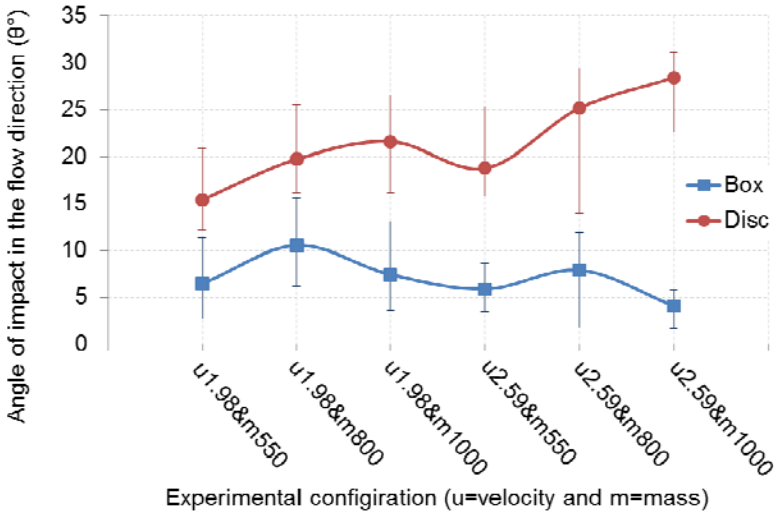


Figure 2 - Relation between impact angle and experimental configuration

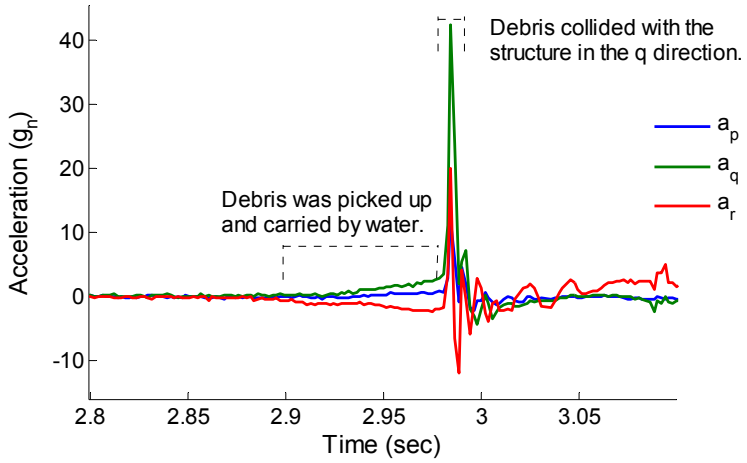


Figure 3 - Sample run of the smart debris device (the disc). The impact is in the accelerometer q direction.

Acceleration at a point of a continuous medium of an object is related to its velocity and displacement by simple relationships that are a single or double integration, respectively. This method is frequently used in strong-motion earthquake research to acquire the structure displacement from ground motion acceleration. It is widely recognised that velocity results cannot be obtained by simple integration without pre-processing of the acceleration data (Boore, 2005, Yang et al, 2006, Stiros, 2008, Chen et al, 2010). Direct integration of acceleration records often causes unrealistic drifts in displacements and velocities (Yang et al, 2006).

Direct integration of acceleration results in a large positive or negative drift. In order to overcome this problem, very low frequency components were filtered out first from the raw acceleration data. The acceleration was then converted to velocity through a single integration. To remove low frequency components, a Butterworth filter was applied to the acceleration data using the Matlab function *butter*. The Butterworth filter is the best compromise between attenuation and phase response. A filtering order and a normalized cut-off frequency were needed to be included as the component values of the filter in the butter function. The filtering order and normalized cut-off frequency were chosen to be 4 and 0.22 Hz in this study. A simple test was designed to determine these values. A carriage was made using a Plexiglas sheet with attached ball bearings for easier movement. The carriage was connected to a rotary motor through a metal arm to transform the motor movement to the carriage. The accelerometer was tightly screwed to the carriage and subjected to a sinusoidal motion over 234 mm distance. The motor speed was adjustable from low to high frequencies. The time the carriage travelled the distance of 234 mm was recorded to calculate the average velocity of the motion. The test was repeated for three different speeds of 0.22, 0.64 and 1.04 m/s. It was revealed that the cut-off frequency value was independent of velocity variation and the value of 0.22 Hz results in a fairly accurate estimation of the debris velocity from acceleration filtered-data. The designed Butterworth filter was applied to the real-test acceleration data to obtain the smart debris velocities during different experiments. Also, the smart debris velocities in some runs were estimated from video snapshots and compared with this method. There was good agreement between the two velocities, confirming the validity of the integration method. Figure 4 shows the relation between experimental configuration and debris velocities derived from single integration of the accelerations.

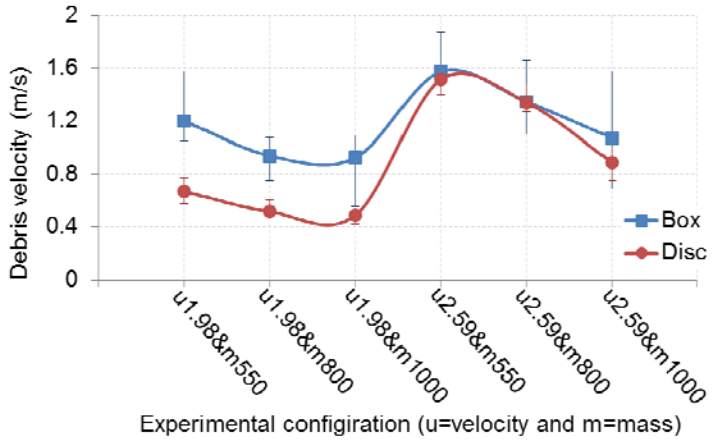


Figure 4 - Relation between debris velocity and experimental configuration

From Figure 4 it can be concluded that, as expected, the debris velocity increased with increasing bore velocity. Acceleration and velocity of the smart debris are both proportional to the kinetic energy of the bore. A faster bore has larger kinetic energy and applies a larger force to the initially stationary smart debris; it accelerates the smart debris more than a slower bore, resulting in higher velocity of the floating smart debris and a faster movement of the floating object. The smart debris velocity decreases with increasing debris mass. Kinetic energy is proportional to the mass; for the same amount of energy transferred to an object, an object with larger mass will attain a lower velocity. It was also observed that, for all configurations, the disc velocity was less than the box velocity. The disc and box have the same projected area but the disc is more streamlined than the box and hence receives less initial force from the water when it is picked up. Also, the box has a longer length exposed to the drag force from water flowing around the smart debris.

Figure 5(a) presents an idealised representation of the acceleration profile recorded by the smart debris, where $\Delta t$ is the contact duration and $t_r$ is the impact rise time. Figure 5(b) shows the contact duration of the disc and box for each combination of mass and bore velocity.

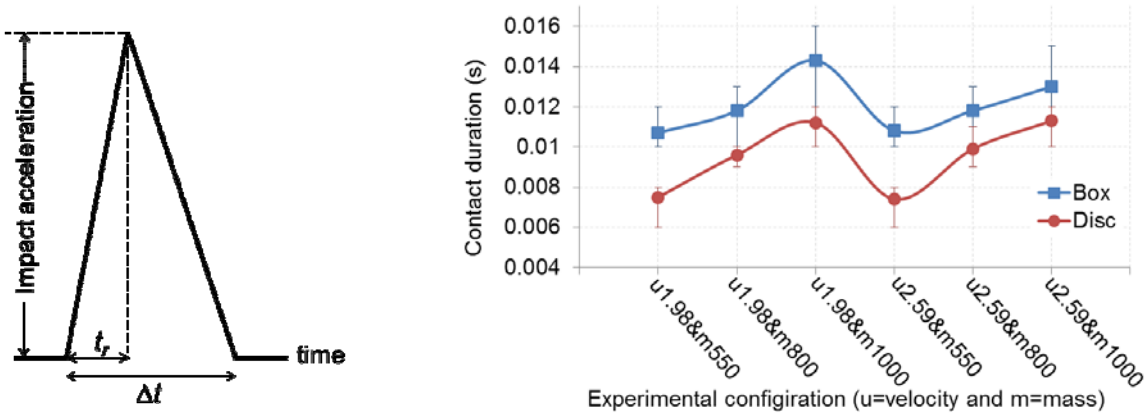


(a) (b)

Figure 5 - (a) Acceleration profile. (b) Contact duration ($\Delta t$) vs. experimental configuration

In the disc collision, the average contact duration from the accelerometer record varied between 7.5 and 11.5 ms and the initial rise time in the acceleration ranged from 3 to 5 ms. Video image analysis also confirmed these values for $\Delta t$ and $t_r$. For the box collision, the contact duration was 11 to 14.5 ms and the initial rise time was between 5 to 7 ms. The results show that the contact time increases as the mass of the object increases. It was also found that the contact duration was independent of the debris velocity. A larger mass of the smart debris took longer to accelerate and move off the structure, thereby increasing the contact duration.

Figure 6(a) shows the impact acceleration for each experimental configuration; Figure 6(b) compares the accelerations of the disc and box collisions, in the flow direction, respectively.

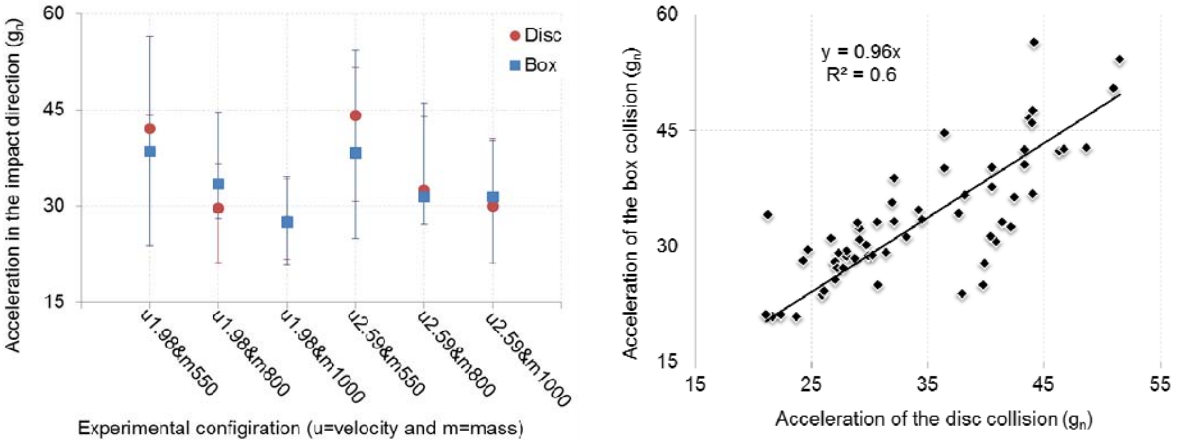


(a) (b)

Figure 6 - (a) Impact acceleration vs. experimental configuration. (b) Impact acceleration of the disc vs. the box collisions.

The variation in the acceleration readings occurred because the debris had variable orientations and did not always collide with the structure at the contact point. The accelerations of the disc collision were, on average, slightly larger than those for the box. This shows that the object geometry was not the only parameter that can affect the impact acceleration. The point on the structure where the debris strikes it and the angle of the debris at the instant of impact are the key parameters affecting the impact acceleration. Also, the amount of water trapped between the debris and the structure can significantly contribute to damping of the impact acceleration. Therefore, variation in the impact acceleration was to be expected because of experimental variability in the floating object impacts resulting from water fluctuations and the other parameters discussed immediately above. The acceleration data from this experiment were used to calculate the debris impact force ($F_{di}$), using the impulse momentum approach (Eq. (1)):

$$F_{di} = m_t a_{di} \quad (1)$$

$$m_t = m_d + m_{add} \quad (2)$$

where $a_{di}$ is the debris impact acceleration and $m_t$ is the total mass which is the summation of the debris mass ($m_d$) and an added mass of water ($m_{add}$). The added mass is the mass of water entrained by the moving object and depends on the shape of the object, its orientation as it moves through the water, and the degree of submergence. Therefore, the added mass of a simple geometric shape can be formulated in the form of Eq. (3):

$$m_{add} = \rho V_{sub} \quad (3)$$

$$V_{sub} = V_d \left( \frac{\rho_d}{\rho_w} \right) \quad (4)$$

in which $V_{sub}$ is the submerged volume of the debris (calculated using Archimedes' principle), $V_d$ is the total volume of the smart debris, $\rho_d$ is the density of the debris and $\rho_w$ is the water density. From video snapshots analysis it was observed that the percentage of the object submergence a few second before the impact instant was more than the calculated one from Eq. (4). Therefore, a coefficient of $\sigma_V$=1.4 was added to the Archimedes' equation to calculate the percentage of the object submergence. This coefficient was derived from video snapshots. Table 1 shows the different values of $\beta_V$ (= $V_{sub}/V_d$) that were adopted for different masses of the disc and the box. The box density is 50% less than the disc and subsequently resulted in smaller values of $V_{sub}$.

Table 1 Values of $\beta_V$, the ratio of the $V_{sub}$ to the $V_d$

| **Debris** | **Disc** | | | **Box** | | |
|---|---|---|---|---|---|---|
| | **550 g** | **800 g** | **1000 g** | **550 g** | **800 g** | **1000 g** |
| $\beta_V$ | 0.50 | 0.70 | 0.90 | 0.25 | 0.35 | 0.45 |

The impact orientations were used to resolve the acceleration data into the flume horizontal (xy) plane (normal to the face of the structure) and the vertical (z) direction. The impact forces $F_{xy}$ and $F_z$ were calculated from these accelerations using Eq. (1). The image processing technique used herein is a 2D method to detect the impact angle in the xz plane of the flume. Therefore, the resultant force was calculated in the horizontal plane to eliminate the possible error of tilting the object in the yz plane of the flume. Figures 7(a) and 7(b) show the debris impact forces in the horizontal plane and the vertical direction, respectively. $F_{xy}$ and $F_z$ both increase with increasing debris velocity and debris mass.

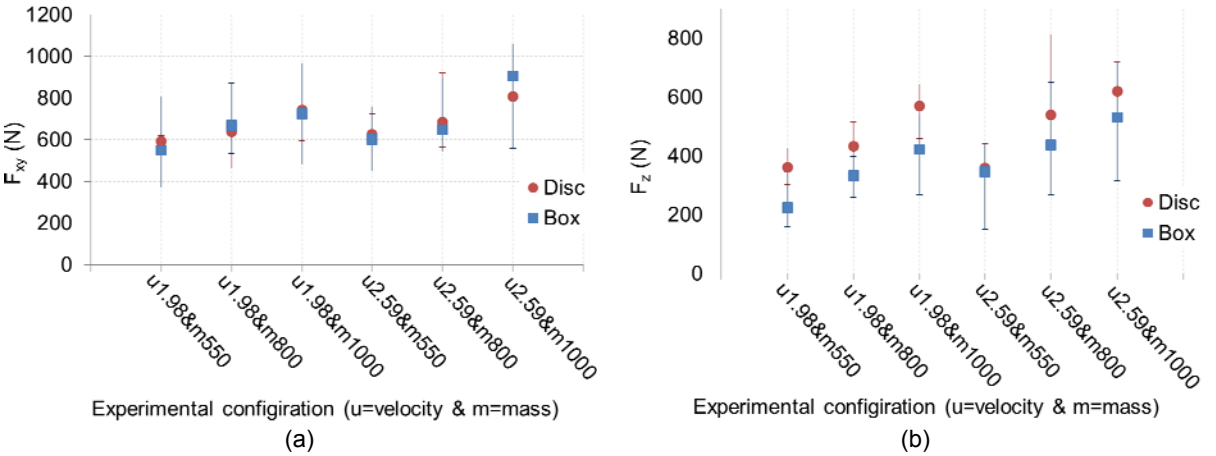


Figure 7 - Debris impact force: (a) in the horizontal plane and (b) in the vertical direction.

Although the disc had slightly larger impact acceleration in the direction of collision, both debris models resulted in a similar range of forces in the horizontal plane. The box collided with the structure at smaller angles than the disc and so a substantial part of the applied forces acted in the horizontal plane, while for the disc collision part of the applied forces acted in the vertical direction. The vertical

component of the force is the result of frictional force which applies to the structure surface in the vertical direction. This force depends on the rigidity of the structure and potentially surface deformation on impact, and may reduce with increasing the rigidity of the cladding material. This method of measuring accelerations using a smart debris device allows direct estimation of the force applied to the structure surface at the instant of collision. This force at the structure surface can concentrate the debris impact on the cladding material and result in a punching force that can damage a small area.

## 4. CONCLUSIONS

The impact force of floating objects on a structure, representative of tsunami-borne debris, was investigated. The force was measured at the contact point of the collision using the smart debris device. The smart debris device was either a disc- or a box-shaped object, representative of two generalised geometrical shapes. The experiments were conducted with two different tsunami bore velocities (1.98 m/s and 2.59 m/s), and, for each velocity and debris shape, for different masses of object (550 g, 800 g and 1000 g) . The acceleration data recorded by the smart debris device were used to calculate the impact force of the debris. Impact orientation was estimated using an image processing technique.

The added mass has a significant effect on the impact force of tsunami borne debris. The effect of some other parameters of impact such as impact angle, contact duration, debris mass and velocity, were investigated. The contact duration was 7.5 to 11.5 ms for the disc and 11 to 14.5 ms for the box collisions. The impact on the central section of the structure produced considerable forces in the horizontal and vertical planes.

## 5. ACKNOWLEDGEMENT

The study is funded by the New Zealand Ministry of Business, Innovation and Employment, through GNS Science.

## 6. REFERENCES

ASCE 7 (2006), Minimum design loads for buildings and other structures, ASCE/SEI 7-05.

Boore, D. M. (2005), Long-period ground motions from digital acceleration recordings: a new era in engineering seismology, Directions in Strong Motion Instrumentation, Springer, 41-54.

Chen, T., Hu, W. and Sun, R. (2010), Displacement Measurement Algorithm Using Handheld Device with Accelerometer, 2010 Asia-Pacific Conference on Wearable Computing Systems (APWCS), IEEE, 122-126.

FEMA (2011), Coastal Construction Manual, Volume 2, Technical Report for the Federal Emergency Management Agency, 400 pages.

Ghobarah, A., Saatcioglu, M. and Nistor, I. (2006), The impact of the 26 December 2004 earthquake and tsunami on structures and infrastructure, Engineering Structures, 28 (2), 312-326.

Haehnel, R. B. and Daly, S. F. (2004), Maximum Impact Force of Woody Debris on Floodplain Structures, Journal of Hydraulic Engineering, 130 (2), 112-120.

Lukkunaprasit, P. and Ruangrassamee, A. (2008), Building damage in Thailand in the 2004 Indian Ocean tsunami and clues for tsunami-resistant design, The IES Journal Part A: Civil & Structural Engineering, 1 (1), 17 - 30.

Madurapperuma, M. A. and Wijeyewickrema, A. C. (2012), Inelastic dynamic analysis of an RC building impacted by a tsunami water-borne shipping container, Journal of Earthquake and Tsunami, 6 (01),

Matsutomi, H. (2009), Method for Estimating Collision Force of Driftwood Accompanying Tsunami Inundation Flow, Journal of Disaster Research, Vol.4 (No.6), 435-440.

Mizutani, N., Gyeong-Seon, Y. and Usami, A. (2008), Estimation of Collision Force of a Drifted Container due to Run-up Tsunami, International Society of Offshore and Polar Engineers, Cupertino, CA, 95015-0189, USA.

Nouri, Y., Nistor, I. and Palermo, D. (2010), Experimental investigation of tsunami impact on free standing structures, Coastal Engineering Journal, 52 (1), 43-70.

Saatçioğlu, M. (2009), Performance of Structures During the 2004 Indian Ocean Tsunami and Tsunami Induced Forces for Structural Design, Earthquakes and Tsunamis, Springer, 153-178.

Stiros, S. C. (2008), Errors in velocities and displacements deduced from accelerographs: An approach based on the theory of error propagation, Soil Dynamics and Earthquake Engineering, 28 (5), 415-420.

Thomas, S. A. (2010), Developing tools to improve tsunami resilient design of coastal structures, Oregon State University.

Yang, J., Li, J. and Lin, G. (2006), A simple approach to integration of acceleration data for dynamic soil–structure interaction analysis, Soil Dynamics and Earthquake Engineering, 26 (8), 725-734.

Yeh, H., Robertson, I. and Preuss, J. (2005), Development of design guidelines for structures that serve as tsunami vertical evacuation sites, NATURA.

Yeom, G. S., Nakamura, T. and Mizutani, N. (2009), Collision analysis of container drifted by runup tsunami using drift collision coupled model, Journal of Disaster Research, 4 (6), 441-449.